ISSN 0965-545X, Polymer Science, Ser. A, 2014, Vol. 56, No. 4, pp. 558–567. © Pleiades Publishing, Ltd., 2014.
Original Russian Text © S.G. Fal'kovich, S.V. Larin, V.M. Nazarychev, I.V. Volgin, A.A. Gurtovenko, A.V. Lyulin, S.V. Lyulin, 2014, published in Vysokomolekulyarnye Soedineniya. Ser. A, 2014, Vol. 56, No. 4, pp. 478–488.

Computer Simulation of the Heat-Resistant Polyimides ULTEM™ and EXTEM™ with the Use of GROMOS53a6 and AMBER99 Force Fields

S. G. Fal'kovich[a], S. V. Larin[a], V. M. Nazarychev[a], I. V. Volgin[b], A. A. Gurtovenko[a,b], A. V. Lyulin[c], and S. V. Lyulin[a,b,*]

[a] *Institute of Macromolecular Compounds, Russian Academy of Sciences, Bol'shoi pr. 31 (V.O.), St. Petersburg, 199004 Russia*
[b] *St. Petersburg State University, Ul'yanovskaya ul. 1, Petrodvorets, St. Petersburg, 198504 Russia*
[c] *Department of Applied Physics, Eindhoven University of Technology, PO Box 513, 5600 MB Eindhoven, Netherlands*
**e-mail: s.v.lyulin@gmail.com*

Received August 15, 2013;
Revised Manuscript Received January 23, 2014

Abstract—An atomistic computer simulation was performed for the polyimides ULTEM™ and EXTEM™ via the molecular-dynamics method with the use of Gromos53a6 and Amber99 force fields. For parameterization of electrostatic interactions, the partial atomic charges were calculated through quantum-chemical methods. The temperature dependence of density and the thermal-expansion coefficients for the polyimides were obtained. The calculated density values of the polyimides at room temperature and their coefficients of thermal expansion in the glassy state are in agreement with available experimental data. It is shown that inclusion of electrostatic interactions is necessary for simulation of the thermophysical characteristics of the considered polyimides.

DOI: 10.1134/S0965545X14040063

INTRODUCTION

Polyimides (PIs) are a class of heat-resistant polymers commonly used to create modern construction materials in the automotive, and aerospace industries. They are of great interest because PI-based materials possess improved thermostability and thermoresistance as well as strength and durability comparable to those of metals, while such materials have lower specific weight [1–4]. It is well known that even small variations in the chemical structure of PIs can substantially influence the physical properties of PI-based materials [5, 6]. Therefore, the synthesis of new PIs with specified features requires an understanding of the relationship between their properties and chemical structure.

One of the most effective methods to solve this problem is an atomistic computer simulation [7–9]. Most studies of the computer simulation of PIs are devoted to the molecular mechanisms of the gas permeability of polyimide films [5, 6, 10–28]. At the same time, studies involving investigation of computer-simulation methods for examining the thermal properties of PIs are relatively rare [29–34], although such methods are used to determine the permissible operating regimes for final PI-based products. In the context of this topic, choosing a model and simulation methods that make it possible to describe the thermophysical properties of polyimides adequately is fundamentally important. In our previous studies [30–34] molecular-dynamics simulations of a number of heat-resistant PIs were carried out and the thermal properties of these materials were studied. It was shown that it is necessary to simulate melts in the microsecond time scale for equilibration of systems consisting of even relatively short polymer chains with a degree of polymerization of $n = 8$ [31–33]. Such a simulation is accomplished only with a software package optimized for use on multiprocessor super computers.

The optimal choice for such resource-intensive computing is the Gromacs package [35, 36], which is used in the present study. The glass-transition temperatures and coefficients of thermal expansion of PIs reproduce qualitatively experimental data, while somewhat different in value, were calculated in [30–32, 34] with the use of the Gromos53a6 force field [37]. The non-optimal choice of the force field (a set of parameters for describing interactions in the simulated system) may be one of the possible causes of discrepancies in the results. To determine the influence of the force field on the correctness of the simulation of PIs, it is necessary to perform comparative modeling of PIs the same chemical structures in various force fields.

Atomistic computer simulations take into account excluded volume, covalent, and electrostatic interactions between individual atoms. The force fields

included in the Gromacs package include the parameters for describing covalent bonds between atoms and the valence and dihedral angles as well as the parameters of excluded volume interactions between unbound atoms. Force-field parameters are chosen so that the computer simulation can reproduce the known experimental characteristics for the test set of molecules. For comparison, we used the Amber [38] and Gromos [37] families of force fields. They were designed in such way that conformational energy values (Amber) or heats of vaporization and solvation (Gromos) were reproduced for a given set of molecules. These force fields were chosen because of the differences in the approach used for parameterization, in particular, for the calculation of partial atomic charges (this will be discussed below).

Correct consideration of electrostatic interactions in the computer simulation is a fairly complex task. Above all, consideration for the long-range electrostatic interactions leads to a significant slowdown of relaxation processes occurring in the system [32, 33] and the simulation itself. Moreover, simulation of new compounds requires determination of the partial atomic charges, which are calculated through quantum-chemical methods. For compounds with large numbers of atoms (several dozens) such calculations are time- and resource-demanding. The question of the choice of the calculation method for partial charges remains unsolved. Thus, compared to a simulation without electrostatic interactions, a computer simulation with electrostatic full-atom interactions is accompanied by a high cost of computing resources and a number of methodological problems.

Note that there have been studies involving the simulation of polymer melts without consideration for electrostatic interactions, i.e., with partial charges equal to zero [39–41]. At the same time, the correctness of this approach for polymers containing polar groups, in particular, PIs, remains still open question. If the physical properties of the polyimides are highly affected by electrostatic interactions between atoms, rather than chain flexibility and free volume [42, 43], rejection of their consideration should lead to poorer agreement between simulation results and experimental data.

In this study, the industrial thermoplastic polyimides ULTEM™ and EXTEM™ (SABIC Innovative Plastics) were chosen as objects of the research.

Monomer units of these polymers contain identical dianhydride fragments, but different diamine ones.

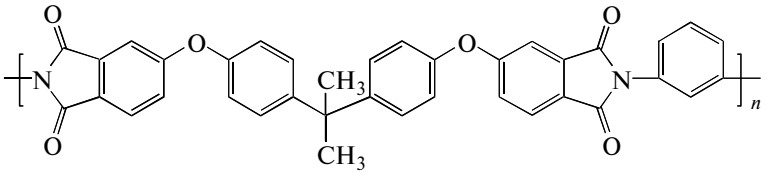

ULTEM™

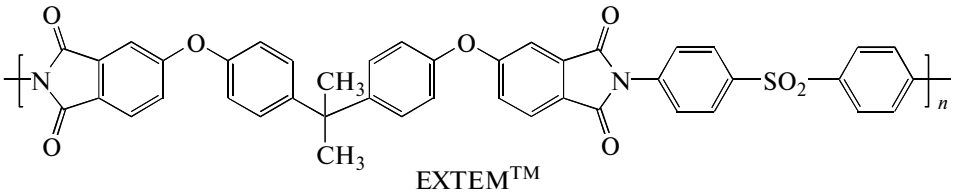

EXTEM™

The difference is the following: the diamine part of ULTEM™ consists of a benzene ring in the meta position, while the diamine part of EXTEM™ consists of a diphenylsulfone group. The dianhydride fragments of both polyimides, as well as the diphenylsulfone group in EXTEM™, contain highly polarized atoms. It was shown previously [30, 32] that the presence of a sulfone group with highest values of partial charges in a PI repeating unit has a significant influence on its structure and properties. Therefore it can be assumed that electrostatic interactions mainly determine the physical properties of ULTEM™ and EXTEM™. They are substantially different at similar values of molecular mass, which are 5.5×10^4 and 4.1×10^4 g/mol, respectively, in the experiment [44–47]. The difference in glass-transition temperatures T_g of the polyimides is ~50°C (for ULTEM™, $T_g = 218$°C; for EXTEM™, $T_g = 267$°C). Furthermore, their densities differ at room temperature (1300 and 1270 kg/m^3 for EXTEM™ and ULTEM™, respectively). At the same time, the experimentally determined values of coefficients of thermal-expansion (CTEs) are close one to another. For ULTEM™, the CTE is 1.65×10^{-4} 1/K [46]; for EXTEM™, the CTE is 1.5×10^{-4} 1/K [47]. The similar CTEs of the polyimides either are due to the fact that the electrostatic interaction is not substantial for this characteristic or are

determined by a combined contribution of various factors, such as electrostatic interaction and the flexibility and mobility of polymer chains. If the electrostatic interaction does not affect the CTEs of polyimides, it may be determined via a computer simulation without electrostatic interactions. To answer the question about the need of including electrostatic interactions in the simulation of PIs, we carried out simulations both with and without consideration for electrostatic interactions.

The CTE was chosen as the parameter to be used in estimating the agreement between the results of the simulation and the experimental data because the accurate determination of the glass-transition temperature via computer simulation is rather complicated [32, 34]. In the simulation, the temperature dependence of polyimide density, $\rho(T)$, which is the basis for calculation of the thermal characteristics of polyimides, is obtained via cooling of polymer systems at a rate 10–15 orders higher than the cooling rate in an experiment [48–50]. This circumstance makes it impossible to reliably determine the dependence of the thermophysical properties of PIs, including the glass-transition temperature, on the cooling rate. At the same time, the CTE determined from the slope of $\rho(T)$ in the area corresponding to the glassy state of the polymer is almost independent on the cooling rate [34, 40].

The goals of this study are to select a better force field for PIs simulation and to examine the effect of electrostatic interactions on the coefficients of thermal expansion T.

MODEL AND SIMULATION METHOD

The simulation of the polyimides ULTEM™ and EXTEM™ via full-atom molecular dynamics was performed with consideration non-bonded interactions between atoms, covalent interactions (covalent bonds, valent and dihedral angles), and electrostatic interactions. The widely used Amber99 [38] and Gromos53a6 [37] force fields were applied. The Gromos53a6 force field performed well in our previous papers devoted to simulation of PIs [30–34]. Modeling of PIs with the Amber99 force field allowed a reliable reproduction of their mechanical characteristics in comparison with the OPLS-AA and MM3 force fields [51].

The Amber99 force-field parameters were supplemented with the EXTEM™ parameters necessary for description of the sulfone group, which were taken from the GAFF (generalized Amber force field) [52]. This approach is possible because of the common form of the interaction-potential functions for these fields and the presence of the atomic types required for parameterization of test compounds. A similar approach was used earlier when the parameters of the Amber99 force field were not sufficient for description of the studied systems [53].

The standard method of calculation of partial charges is not determined for the force fields of the Gromos family. As in our previous studies [32–34], calculation of the partial atomic charges of PIs via the Gromos53a6 force-field simulation were performed through the Hartree–Fock approach with the use of the 6-31G* basis functional set and the Mulliken method.

It is recommended for the force fields of the Amber family to calculate the partial atomic charges via the restricted electrostatic-potential (RESP) method with the 6-31G* basis set of wave functions [38]. However, the large numbers of atoms in the repeating units of ULTEM™ and EXTEM™ make it difficult to apply the RESP for calculation of their partial charges, because of the high demands of this method for computer resources. For this reason, the semi-empirical AM1-BCC method [54] was used; it is employed to calculate partial atomic charges in large molecules and makes it possible to obtain results analogous to those found via the RESP method, but with less consumption of computer resources [52]. The AM1-BCC method of calculating the charges includes simultaneous consideration for formal atomic charges, consideration for the specifics of the electron distribution in a molecule, including π delocalization, and subsequent corrections for atoms bonded to each other (bond-charge corrections).

In this paper, PI samples containing 27 chains with a degree of polymerization of $n = 9$, which corresponds to number-average molecular weight of $M \sim 6 \times 10^3$, were simulated. This molecular weight corresponds to the beginning of the "polymeric regime," which is characterized by insignificant variation in the glass-transition temperature of a polymer sample with a further increase of its molecular weight [30, 34, 55].

The simulation was performed under periodic boundary conditions with the use of the NpT ensemble. The accepted average values of temperature and pressure were maintained by the Berendsen thermostat and barostat [56, 57], which allowed rapid quenching of fluctuations of temperature and pressure and operated well in our previous studies where the thermal properties of PIs were investigated [30–34]. Electrostatic interactions were taken into account via the Ewald summation method with the use of the PME algorithm [58].

Generation of the initial system configuration and the preliminary equilibration of the system, which comprised the steps of compression and thermal annealing, were performed according to the procedure approved in [30–34].

The total duration of the preliminary stage of equilibration was 100 ns. After the annealing, the simulation was performed for ~3 μs at a pressure of 1 bar and a tem-

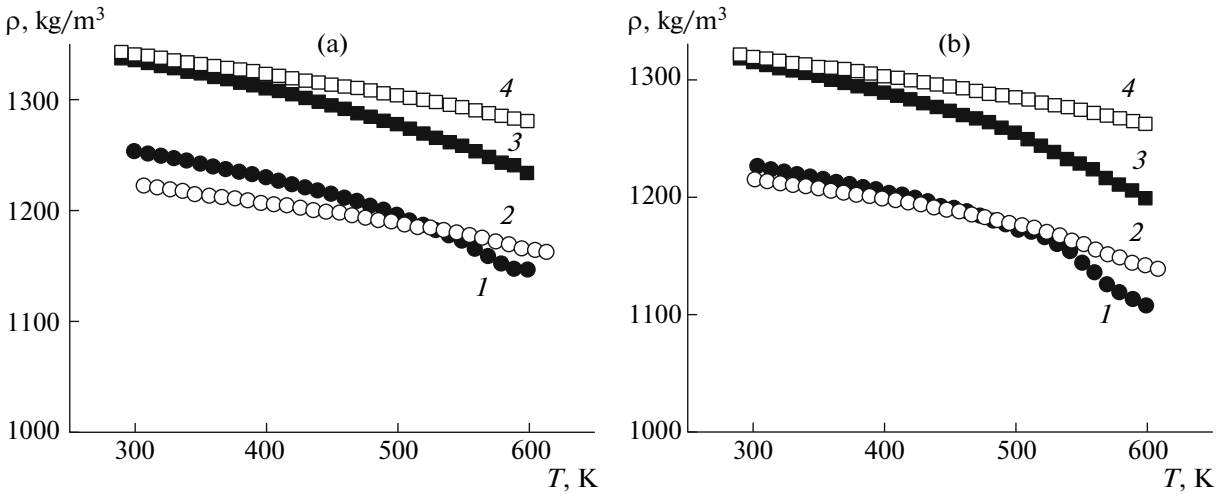

Fig. 1. Temperature dependence of the densities of (a) EXTEM™ and (b) ULTEM™ at a cooling rate 1.5×10^{12} K/min that were obtained via simulation with the (*1*, *2*) Amber99 and (*3*, *4*) Gromos53a6 force fields (*2*, *4*) with and (*1*, *3*) without electrostatic interactions.

perature of 600 K, which exceeded experimental values of the glass-transition temperatures of the examined PIs. A long simulation is necessary because the equilibration times of PI melts, which is characterized by the diffusion of the polymer chains for a distance comparable to their own sizes, are ~1 μs or longer [31–33].

To determine the thermal characteristics of the PIs, stepwise cooling was carried out for 11 independent configurations of ULTEM™ and EXTEM™ prepared under equilibration of uncharged systems in the Gromos53a6 force field and for 5 independent configurations obtained under equilibration of uncharged systems in the Amber99 force field. Temperature was lowered abruptly by 10 K at each cooling step; then, equilibration was performed for 400 ps, while the average cooling rate was 1.5×10^{12} K/min. This procedure of stepwise cooling for the simulation of thermal properties was tested earlier in A.V. Lyulin's studies [39, 40]. There, it was shown, in particular, that continuous cooling led to worse reproduction of experimental results than stepwise cooling did. In addition, stepwise cooling was explored in our investigations of the thermal properties of PIs [30–32, 34].

Before the simulation of cooling for the systems with consideration for electrostatic interactions, as in [32–34], for each of the selected PI configurations obtained during equilibration without electrostatic interactions, equilibration was performed at 600 K for 100 ns with electrostatic interactions. The resulting cooling curves were further averaged, and the relative deviation of density did not exceed 0.5%.

RESULTS AND DISCUSSION

The temperature dependence of the densities of the PIs are shown in Fig. 1. There are two parts on the cooling curves where the temperature dependence of density are close to linear. A region with a larger angle located at higher temperature values corresponds to high elastic state of a PI. During cooling of a system, the polyimide transitioned from the visco-elastic state to the glassy state, which corresponds to the low-temperature linear part of the $\rho(T)$ curve with a smaller slope at lower temperatures. Note that the slopes of the two regions of cooling curves obtained in the simulation with electrostatic interactions are slightly different. Such behavior of systems is due to the fact that chain mobility slows significantly by the influence of dipole–dipole interactions [32–34]. This effect is particularly strong for EXTEM™, which contains a polar sulfone group. The partial charges at the sulfur atom in the sulfone group are 1.59 and 1.49 for the Gromos53a6 and Amber99 force fields, respectively. The partial atomic charges at an oxygen in the sulfone group are −0.70 for Gromos53a6 and −0.66 for Amber99. For comparison, the partial atomic charges of sulfur and oxygen in Sulfur Dioxide are 1.56 and −0.78, respectively [59]. Full lists of the partial atomic charges for the considered PIs are shown in Tables 1 and 2, and below, the configurations of monomer units of EXTEM™ and ULTEM™ with identification designations of atoms are given.

Table 1. Partial atomic charges of the polyimide EXTEM^{TM} calculated via the HF/6-31G* method for the Gromos53a6 force field and via the AM1-BCC method for the Amber99 force field

Atom identifier	Partial charge		Atom identifier	Partial charge	
	HF/6-31G*	AM1-BCC		HF/6-31G*	AM1-BCC
CAF	−0.145	−0.078	HBG	0.215	0.182
HAF	0.212	0.180	CBM	−0.207	−0.185
CAC	−0.137	−0.110	HBM	0.189	0.162
CAB	0.828	0.725	CBL	−0.089	−0.020
OAJ	−0.547	−0.564	HBL	0.204	0.166
NAA	−0.818	−0.522	CBI	−0.177	−0.176
CAE	0.829	0.731	CBE	0.857	0.739
OAK	−0.555	−0.570	OBF	−0.553	−0.548
CAD	−0.177	−0.172	CBJ	−0.136	−0.110
CAI	−0.092	−0.026	CBH	0.857	0.733
HAI	0.201	0.164	OBC	−0.544	−0.555
CAH	−0.207	−0.185	NBD	−0.939	−0.434
HAH	0.187	0.160	CBN	0.308	0.125
CAG	0.401	0.138	CBS	−0.120	−0.172
OAL	−0.716	−0.243	HBS	0.190	0.169
CAM	0.339	0.078	CBR	−0.112	−0.001
CAO	−0.166	−0.139	HBR	0.204	0.156
HAO	0.174	0.153	CBO	−0.123	−0.172
CAP	−0.166	−0.114	HBO	0.191	0.168
HAP	0.162	0.146	CBP	−0.113	0.002
CAN	−0.163	−0.120	HBP	0.204	0.159
HAN	0.176	0.158	CBQ	−0.346	−0.379
CAR	−0.135	−0.110	SBZ	1.587	1.457
HAR	0.166	0.149	OCB	−0.698	−0.663
CAQ	−0.005	−0.071	OCA	−0.697	−0.662
CAS	−0.078	0.042	CBX	−0.345	−0.441
CAU	−0.314	−0.085	CBW	−0.121	0.034
CAV	−0.314	−0.085	HBW	0.204	0.154
CAT	−0.005	−0.064	CBU	−0.130	−0.233
CBA	−0.134	−0.112	HBU	0.190	0.141
HBA	0.167	0.150	CBT	0.297	0.238
CAZ	−0.163	−0.126	CBV	−0.129	−0.233
HA2	0.176	0.155	HBV	0.190	0.141
CAW	−0.166	−0.118	CBY	−0.118	0.036
HA0	0.163	0.147	HBY	0.204	0.152
CAX	−0.165	−0.121	HAU	0.128	0.044
HA1	0.175	0.155	HAV	0.123	0.046
CAY	0.337	0.070	HAW	0.118	0.049
OBB	−0.715	−0.242	HAX	0.122	0.045
CBK	0.403	0.145	HAY	0.119	0.045
CBG	−0.144	−0.076	HAZ	0.127	0.048

Table 2. Partial atomic charges of the polyimide ULTEM^{TM} calculated via the HF/6-31G* method for the Gromos53a6 force field and via the AM1-BCC method for the Amber99 force field

Atom identifier	Partial charge		Atom identifier	Partial charge	
	HF/6-31G*	AM1-BCC		HF/6-31G*	AM1-BCC
CAF	−0.145	−0.064	CAX	−0.163	−0.127
HAF	0.212	0.178	HA1	0.175	0.157
CAC	−0.137	−0.129	CAY	0.339	0.090
CAB	0.828	0.725	OBB	−0.716	−0.239
OAJ	−0.548	−0.560	CBK	0.401	0.135
NAA	−0.819	−0.521	CBG	−0.145	−0.074
CAE	0.829	0.726	HBG	0.213	0.180
OAK	−0.554	−0.563	CBM	−0.208	−0.178
CAD	−0.177	−0.140	HBM	0.185	0.163
CAI	−0.092	−0.052	CBL	−0.091	−0.028
HAI	0.201	0.167	HBL	0.202	0.165
CAH	−0.207	−0.120	CBI	−0.176	−0.168
HAH	0.185	0.164	CBE	0.858	0.737
CAG	0.401	0.102	OBF	−0.554	−0.556
OAL	−0.716	−0.251	CBJ	−0.136	−0.113
CAM	0.339	0.115	CBH	0.856	0.732
CAO	−0.163	−0.187	OBC	−0.549	−0.557
HAO	0.175	0.147	NBD	−0.936	−0.427
CAP	−0.135	−0.092	CBN	0.280	0.095
HAP	0.161	0.143	CBO	−0.095	−0.176
CAN	−0.164	−0.142	HBO	0.198	0.158
HAN	0.174	0.157	CBP	0.270	−0.079
CAR	−0.166	−0.091	HBP	0.155	0.137
HAR	0.163	0.144	CBQ	−0.126	−0.196
CAQ	−0.003	−0.096	HBQ	0.178	0.137
CAS	−0.080	0.045	CBR	−0.177	0.156
CAU	−0.314	−0.085	CBS	−0.122	−0.199
CAV	−0.314	−0.085	HBS	0.178	0.158
CAT	−0.003	−0.077	HAV	0.119	0.045
CBA	−0.166	−0.105	HAW	0.130	0.049
HBA	0.163	0.145	HAU	0.122	0.045
CAZ	−0.165	−0.162	HAX	0.119	0.043
HA2	0.174	0.150	HAY	0.131	0.050
CAW	−0.135	−0.101	HAZ	0.122	0.044
HA0	0.161	0.148	–	–	–

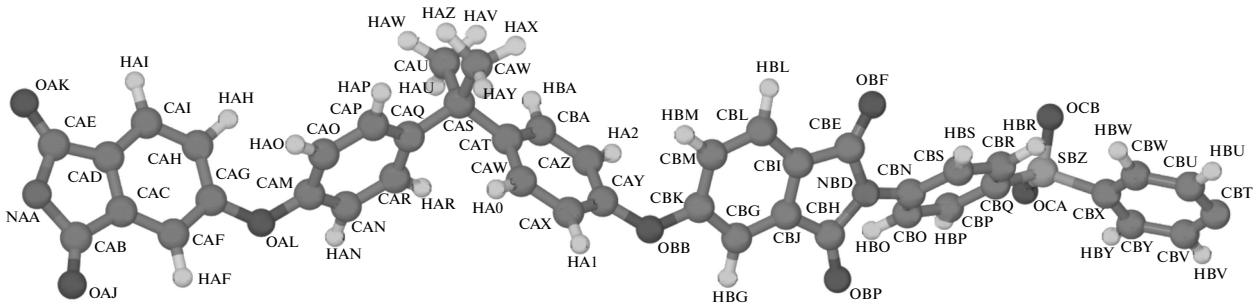

EXTEM™

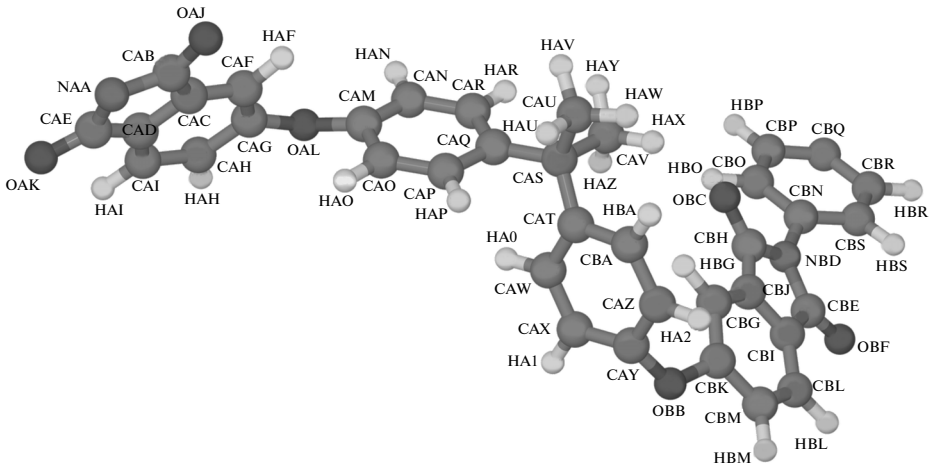

ULTEM™

As shown in Fig. 1, the density of both PIs obtained via calculation with the Amber99 force field (both with and without consideration for electrostatic interactions) were lower than that found with the use of the Gromos53a6 force field. Moreover, the density at room temperature in the simulation with the force field Amber99 was slightly lower than the experimental value, whereas the density in the simulation with the force field Gromos53a6 were slightly higher than the experimental value. In addition, in both cases, the EXTEM™ density was higher than the ULTEM™ density, that agrees qualitatively with the experimental results (Table 3).

The difference in density between EXTEM™ and ULTEM™ is due to the presence of relatively heavy sulfur atoms in the monomer unit of EXTEM™ and stronger dipole–dipole interactions that are characteristic for this PI and is associated with the presence of a strongly polarized sulfone group in the repeating unit. The simulation with consideration for electrostatic interactions should lead to additional compaction of the polymer. As shown earlier in [30], the presence of a sulfone group in the chemical structure of a PI can lead to a decrease in interatomic distances due to the formation of electrostatically stabilized aggregates and, as a consequence, to an increase in the polymer density.

Table 3. Average density values of the EXTEM™ and ULTEM™ polyimides at room temperature according to the results of the computer simulation and experiment

Polyimide	ρ, kg/m^3				Experiment
	Amber99		Gromos53a6		
	with charges	without charges	with charges	without charges	
ULTEM™	1215	1226	1321	1320	1270 [45]
EXTEM™	1222	1253	1340	1340	1300 [46]

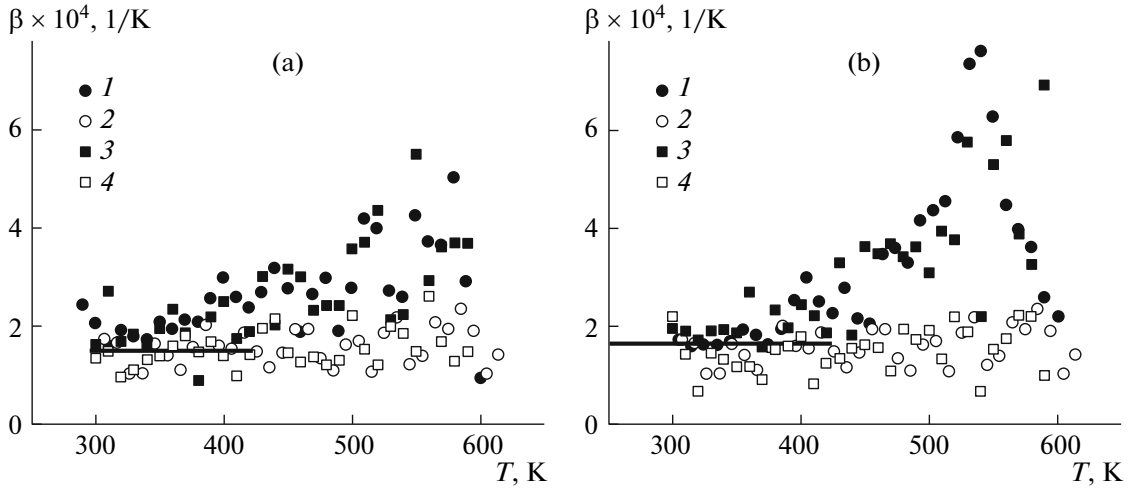

Fig. 2. Temperature dependence of the coefficients of thermal expansion β for (a) EXTEM™ and (b) ULTEM™ at a cooling rate 1.5×10^{12} K/min that were determined from the results of simulations with the (*1*, *2*) Amber99 and (*3*, *4*) Gromos53a6 force fields (*2*, *4*) with and (*1*, *3*) without consideration for electrostatic interactions. The lines show the experimental values of coefficients of thermal expansion in the range 296–423 K for EXTEM™ [46] and in the range 250–423 K for UTLEM™ [45].

The simulation with the Amber99 field with consideration for electrostatic interactions led to a small difference in the densities of the PIs and that compaction occurred only for ULTEM™, whereas the simulation with the Gromos53a6 field afforded compaction of both PIs. When electrostatic interactions were taken into account, compaction of ULTEM™ and EXTEM™ occurred due to dipole–dipole interactions between polarized groups (as mentioned above). However, such compaction may require structural rearrangements that are energetically unfavorable because of presence of the excluded volume at the polymer chains. This factor is especially substantial for EXTEM™, which possesses a bulky sulfone group. Even a small difference in the interaction parameters can shift the balance of the forces; this circumstance is a probable explanation for the difference between the simulation results acquired with the Gromos53a6 and Amber99 fields (Fig. 1).

However, as it will be shown below, such difference have a little effect on the simulation results of the thermophysical properties of ULTEM™ and EXTEM™.

Coefficients of thermal-expansion for the PIs were determined from the cooling curves using the following equation

$$\beta = -\frac{1}{\rho_0}\left(\frac{d\rho}{dT}\right)_p, \quad (1)$$

where ρ_0 is the density of the polyimide system at 300 K. The obtained dependence of CTE on temperature, $\beta(T)$, are shown in Fig. 2.

Averaged values of β for ULTEM™ and EXTEM™ are given in Table 4 in the temperature range of 300–420 K, which corresponds to the experimental CTEs.

Figure 2 and Table 4 show that the calculated CTEs for PIs in the glassy state were close to the experimental values during both the simulation with the Gromos53a6 force field and the simulation with the

Table 4. Average values of the coefficients of thermal expansion for the EXTEM™ and ULTEM™ polyimides in the temperature range 300–420 K according to the results of our computer simulation and the experiment

Polyimide	$\beta \times 10^4$, 1/K				Experiment
	Amber99		Gromos53a6		
	with charges	without charges	with charges	without charges	
ULTEM™	1.5	2.0	1.3	2.0	1.65 [45]
EXTEM™	1.5	2.1	1.4	1.9	1.50 [46]

Amber99 force field. The CTEs determined with electrostatic interactions in the system were lower than the values of CTEs found in simulated systems with zero partial charges.

To quantify the degree of agreement between the data obtained in the simulation and in the experiment we calculated an average (with respect to ULTEM™ and EXTEM™) differences between the values of CTEs obtained in the simulation and the experiment, β_{sim} and β_{exp}:

$$\langle \Delta\beta \rangle = \frac{1}{2}\left(\left|\beta_{sim}^{ULTEM} - \beta_{exp}^{ULTEM}\right| + \left|\beta_{sim}^{EXTEM} - \beta_{exp}^{EXTEM}\right|\right) \quad (2)$$

The $\langle \Delta\beta \rangle$ values are 0.1 and 0.2 with consideration for electrostatic interactions and 0.5 and 0.4 without consideration for electrostatic interactions. The first number in each pair corresponds to the Amber99 force field; the second number in each pair, to the Gromos53a6 force field.

Thus, the results of the simulation with consideration for electrostatic interactions are in better agreement with the experimental data than those without electrostatic interactions. This outcome means that the electrostatic interactions have a significant influence on the thermal properties of polyimides, such as the CTE, and that their consideration is necessary for correct atomistic simulations of PIs. In addition, the presented values of $\langle \Delta\beta \rangle$ indicate that slightly better agreement with the experiment results was obtained during application of the Amber99 field with consideration for electrostatic interactions.

CONCLUSIONS

The results of the computer simulation of the heat-resistant polyimides ULTEM™ and EXTEM™ were compared with the use of two different force fields: Gromos53a6 and Amber99.

The simulation was performed with and without consideration for electrostatic interactions for both of the force fields. The simulation results were used to calculate polymer cooling curves, which were further explored to determine the coefficients of thermal expansion of the polymers in the glassy state.

The coefficients of thermal expansion were similar to the experimental values for both force fields with consideration for electrostatic interactions. Slightly better agreement with the experimental results was achieved in the simulation using the Amber99 force field. It may be concluded that the electrostatic interactions between the polar groups, which are parts of the repeating units of the PIs, mainly determine the thermal properties of the PIs.

Therefore, the correct determination of the thermophysical characteristics of PIs requires obligatory consideration for electrostatic interactions.

ACKNOWLEDGMENTS

In this study, computer simulations were performed with the computer cluster resources of the Institute of Macromolecular Compounds, Russian Academy of Sciences, and on the SKIF Chebyshev and Lomonosov supercomputers of Moscow State University.

This work was supported by the Ministry of Education and Science of the Russian Federation (Agreement no. 8645, State Contract no. 16.523.12.3001).

REFERENCES

1. *Polyimides: A Class of Thermally Stable Polymers*, Ed. by M. I. Bessonov (Nauka, Leningrad, 1983).
2. *Polyimides: Fundamentals and Applications*, Ed. by M. K. Ghash and K. L. Mittal (Marcel Dekker, New York, 1996).
3. H. Ohya, V. V. Kudryavtsev, and S. I. Semenova, *Polyimide Membranes: Applications, Fabrication and Properties* (Tokyo; Amsterdam: Kodansha Ltd., Gordon and Breach Sci. Publ. S.A. (1996).
4. M. J. M. Abadie and A. L. Rusanov, *Practical Guide to Polyimides* (Smithers Rapra Technology, Shawbury, 2007).
5. X.-Y. Wang, P. J. Veld, Y. Lu, B. D. Freeman, and I. C. Sanchez, Polymer **46**, 9155 (2005).
6. J. Xia, S. Liu, P. K. Pallathadka, M. L. Chang, and T. Chung, Ind. Eng. Chem. Res. **49**, 12014 (2010).
7. K. Binder, J. Baschnagel, and W. Paul, Prog. Polym. Sci. **28**, 115 (2003).
8. J.-L. Barrat, J. Baschnagel, and A. Lyulin, Soft Matter **6**, 3430 (2010).
9. K. Binder, *Monte Carlo and Molecular Dynamics Simulations in Polymer Science* (Oxford Univ. Press, Oxford, 1995).
10. S. Neyertz and D. Brown, Macromolecules **41**, 2711 (2008).
11. O. Hölck, M. Heuchel, M. Böhning, and D. J. Hofmann, J. Polym. Sci., Part B: Polym. Phys. **46**, 59 (2008).
12. M. Heuchel, D. Hofmann, and P. Pullumbi, Macromolecules **37**, 201 (2004).
13. S. Neyertz, A. Douanne, and D. Brown, J. Membr. Sci. **280**, 517 (2006).
14. S. Neyertz, A. Douanne, and D. Brown, Macromolecules **38**, 10286 (2005).
15. S. Neyertz and D. Brown, Macromolecules **37**, 10109 (2004).
16. S. Neyertz and D. Brown, Macromolecules **42**, 8521 (2009).
17. S. Pandiyan, D. Brown, S. Neyertz, and N. F. A. Van der Vegt, Macromolecules **43**, 2605 (2010).
18. S. Neyertz, D. Brown, S. Pandiyan, and N. F. A. Van der Vegt, Macromolecules **43**, 7813 (2010).
19. S. Neyertz, Macromol. Theory Simul. **16**, 513 (2007).
20. S. Velioğlu, M. G. Ahunbay, and S. B. Tantekin-Ersolmaz, J. Membr. Sci. **417–418**, 217 (2012).

21. M. Minellia, M. G. De Angelisa, and D. Hofmann, Fluid Phase Equilib. **333**, 87 (2012).
22. Y. Chen, S. P. Huang, Q. L. Liu, I. Broadwell, and A. M. Zhu, J. Appl. Polym. Sci. **120**, 1859 (2011).
23. Y. Chen, Q. L. Liu, A. M. Zhu, Q. G. Zhang, and J. Y. Wu, J. Membr. Sci. **348**, 204 (2010).
24. C. Nagel, E. Schmidtke, K. Günther-Schade, D. Hofmann, D. Fritsch, T. Strunskus, and F. Faupel, Macromolecules **33**, 2242 (2000).
25. D. Hofmann, L. Fritz, J. Ulbrich, C. Schepers, and M. Böhning, Macromol. Theory Simul. **9**, 293 (2000).
26. R. Zhang and W. L. Mattice, J. Membr. Sci. **108**, 15 (1995).
27. D. Hofmann, L. Fritz, J. Ulbrich, and D. Paul, Comput. Theor. Polym. Sci. **10**, 419 (2000).
28. S. Neyertz, Soft Matter **4**, 15 (2007).
29. P. V. Komarov, Y.-T. Chiu, S.-M. Chen, and P. Reineker, Macromol. Theory Simul. **19**, 64 (2010).
30. S. V. Lyulin, S. V. Larin, A. A. Gurtovenko, N. V. Lukasheva, V. E. Yudin, V. M. Svetlichnyi, and A. V. Lyulin, Polym. Sci., Ser. A **54**, 631 (2012).
31. V. M. Nazarychev, S. V. Larin, N. V. Lukasheva, A. D. Glova, and S. V. Lyulin, Polym. Sci. A **55**, 570 (2013).
32. S. V. Lyulin, A. A. Gurtovenko, S. V. Larin, V. M. Nazarychev, and A. V. Lyulin, Macromolecules **46**, 6357 (2013).
33. S. V. Larin, S. G. Falkovich, V. M. Nazarychev, A. A. Gurtovenko, A. Lyulin, and S. V. Lyulin, RSC Adv. **4**, 830 (2014).
34. S. V. Lyulin, S. V. Larin, A. A. Gurtovenko, V. M. Nazarychev, S. G. Falkovich, V. E. Yudin, V. M. Svetlichnyj, I. V. Gofman, and A. V. Lyulin, Soft Matter **10**, 1224 (2014).
35. D. Van Der Spoel, E. Lindahl, B. Hess, G. Groenhof, A. E. Mark, and H. J. C. Berendsen, J. Comput. Chem. **26**, 1701 (2005).
36. B. Hess, C. Kutzner, D. Van der Spoel, and E. Lindahl, J. Comput. Chem. **4**, 435 (2008).
37. C. Oostenbrink, A. Villa, A. E. Mark, and W. F. Van Gunsteren, J. Comput. Chem. **25**, 1656 (2004).
38. J. Wang, P. Cieplak, and P. Kollman, J. Comput. Chem. **21**, 1049 (2000).
39. A. V. Lyulin and M. A. J. Michels, Macromolecules **35**, 1463 (2002).
40. A. V. Lyulin, N. K. Balabaev, and M. A. J. Michels, Macromolecules **36**, 8574 (2003).
41. S. Karanikas and I. G. Economou, Eur. Polym. J. **47**, 735 (2011).
42. I. A. Ronova and M. Bruma, Struct. Chem. **23**, 47 (2012).
43. I. Ronova, Struct. Chem. **21**, 541 (2010).
44. Y. Wang, L. Jiang, T. Matsuurac, T. S. Chung, and S. Goh, J. Membr. Sci. **318**, 217 (2008).
45. N. Peng, T. Chung, and M. Chang, J. Membr. Sci. **360**, 48 (2010).
46. www.sabic-ip.com/gepapp/Plastics/servlet/ProductsAndServices/Product/series?sltPrdline=Ultem&search=Search#searchresults
47. www.sabic-ip.com/gepapp/Plastics/servlet/ProductsAndServices/Product/series?sltPrdline=Extem#searchresults
48. R. Bruning and K. Samwer, Phys. Rev. B: Condens. Matter **46**, 11318 (1992).
49. K. Vollmayr, W. Kob, and K. J. Binder, Chem. Phys. **105**, 4714 (1996).
50. J. Baschnagel, J. Phys.: Condens. Matter **5**, 1597 (1993).
51. P. Valavala, T. Clancy, T. Gates, and G. Odegard, Int. J. Solids Struct. **44**, 1161 (2007).
52. J. Wang, R. M. Wolf, J. W. Caldwell, P. A. Kollman, and D. A. Case, J. Comput. Chem. **25**, 1157 (2004).
53. N. Homeyer, A. H. C. Horn, H. Lanig, and H. Sticht, J. Mol. Model. **12**, 281 (2006).
54. A. Jakalian, B. Bush, D. Jack, and C. Bayly, J. Comput. Chem. **23**, 1623 (2002).
55. J. V. Facinelli, S. L. Gardner, L. Dong, C. L. Sensenich, R. M. Davis, and J. S. Riffle, Macromolecules **29**, 7342 (1996).
56. H. Berendsen, J. Postma, A. DiNola, and J. Haak, J. Chem. Phys. **81**, 3684 (1984).
57. V. L. Golo and K. V. Shaitan, Biofizika **47**, 611 (2002).
58. T. Darden, D. York, and L. Pedersen, J. Chem. Phys. **98**, 10089 (1993).
59. www.chemeddl.org/resources/models360/models.php?pubchem=1119

Translated by I. Titanyuk